NASA TN D-219

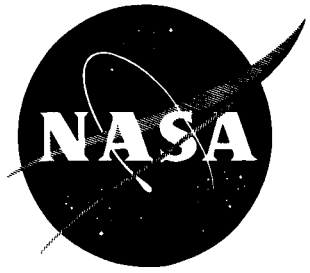

TECHNICAL NOTE
D-219

A THREE-STAGE SOLID-FUEL SOUNDING ROCKET SYSTEM SUITABLE FOR RESEARCH AT ALTITUDES NEAR 200 NAUTICAL MILES

By Waldo L. Dickens and Earl C. Hastings, Jr.

Langley Research Center
Langley Field, Va.

NATIONAL AERONAUTICS AND SPACE ADMINISTRATION

WASHINGTON December 1959

1F

NATIONAL AERONAUTICS AND SPACE ADMINISTRATION

TECHNICAL NOTE D-219

A THREE-STAGE SOLID-FUEL SOUNDING ROCKET SYSTEM SUITABLE FOR RESEARCH AT ALTITUDES NEAR 200 NAUTICAL MILES

By Waldo L. Dickens and Earl C. Hastings, Jr.

L
6
1
0

SUMMARY

A three-stage solid-fuel sounding rocket capable of carrying an 81.5-pound payload to an altitude of 253 nautical miles is discussed. Data from two tests and estimated performance data are presented to show the effects of variation of launch angle, coast time between first-stage burnout and second-stage ignition, and payload weight. The effect of a typical wind profile on performance is also discussed.

INTRODUCTION

The need for test vehicles capable of reaching altitudes of 200 nautical miles or more with payloads in excess of 50 pounds has led to the development of several such vehicles by the Pilotless Aircraft Research Division of the NASA. This paper discusses a solid-fuel three-stage system which has been successfully employed in two tests to boost payloads in the order of 80 pounds to altitudes of over 200 nautical miles. These two tests were conducted at the NASA Wallops Station for the Air Force Cambridge Research Center. The vehicles were designed and constructed by the University of Michigan Research Institute using the concepts and advice of the Langley Pilotless Aircraft Research Division.

Although the two tests were conducted to determine only trajectory information and nose-cone temperature measurements, the vehicles were of a type which has immediate potential for many experimental investigations such as upper atmospheric research, heat transfer, and reentry studies.

This paper presents a description of the vehicles tested, some results obtained from the tests, and a discussion of the calculated effects of payload, launch angle, coast time, and winds on performance of high-altitude research vehicles of this type.

DESCRIPTION OF TEST VEHICLES, INSTRUMENTATION, AND FLIGHT TEST PROGRAMS

Test Vehicles

The two three-stage sounding rockets discussed herein used an Honest John booster, a Nike booster, and a Recruit (XM19E1) solid-fuel rocket motor as the first, second, and third stages, respectively. A drawing of the assembled second test vehicle is presented in figure 1, and a photograph of this vehicle on the launcher is shown in figure 2. Both of the vehicles tested flew ballistic trajectories (no guidance), and no artificial stabilization was employed. With the exception of the nose-cone afterbody length and nose-cone weight, the two test vehicles were identical. The following table presents the weights of the components involved:

Component	Weight, lb
First stage	
Honest John booster motor, loaded	3,783
Fin assembly	252
Adapter, Honest John to Nike	41
Launcher fittings	6
Total, loaded	4,082
Second stage	
Nike booster motor, loaded	1,170.0
Fin assembly	76.5
Adapter, Nike to Recruit	14.8
Total, loaded	1,261.3
Third stage	
Recruit motor (XM19E1), loaded	337.9
Flare	15.4
Nose cone (model 1)	83.5
Nose cone (model 2)	81.5
Total, loaded (model 1)	436.8
Total, loaded (model 2)	434.8

With the exception of the nose-cone package and instrumentation, all of the components used in the tests were "off the shelf" items of proven reliability. The first-stage fins were production military Honest John fins mounted at an angle of incidence of 0°. The second-stage fin assemblies were 2.50 square feet per panel units with Inconel leading-edge cap strips to protect the panels from high temperatures due to aerodynamic heating. Because of the high velocities and temperatures encountered by the third stage, a 10° half-angle conical frustum was used rather than fins as a stabilizing surface for this stage. Dimensions of the fins, flare, and adapters are shown in figure 1. These components were fabricated from standardized designs used by the Langley Pilotless Aircraft Research Division.

The nose cones of models 1 and 2 were designed and constructed by the University of Michigan Research Institute and were attached as an integral unit to the forward face of the third stage. These nose cones, which housed the instrument packages, were truncated 4.3° half-angle cones with 9.0-inch-diameter cylindrical afterbodies. Model 1 had an afterbody length of 7.5 inches and model 2 had an afterbody length of 9.5 inches.

Instrumentation

Instrumentation of models 1 and 2 included accelerometers mounted in the X, Y, and Z directions and temperature elements mounted on the nose cone and inside the nose-cone heat shield. Data from these instruments were transmitted in flight and recorded at the ground receiving station. Telemeter installation and data analysis were done under the supervision of the Air Force Cambridge Research Center. Telemetered data obtained from these tests will not be published by NASA and are the property of the Air Force Cambridge Research Center.

Space and velocimeter radar units at NASA Wallops Station were used in both tests as was the Millstone Hill experimental radar of the M.I.T. Lincoln Laboratory. Ambient atmospheric conditions and wind velocity and direction at the lower altitudes were determined, immediately before the tests, with rawinsonde balloons released from NASA Wallops Station.

Flight Test Programs

Model 1 had a payload of 83.5 pounds and was launched at an angle of 75°; model 2 had a payload of 81.5 pounds and was launched at 80°. Following the first boosted phase, the burned-out Honest John booster stage drag separated from the remaining two stages. The second and third stages coasted 25.0 seconds before second-stage ignition took place.

To prevent premature separation of the second and third stages during the coast period, these stages were locked together with a thin diaphragm (of the type shown in ref. 1) threaded to both the third-stage nozzle and the adapter coupling mounted to the second-stage headcap. When the third-stage rocket motor fired, the thrust pressure collapsed this diaphragm and unlocked the burned-out second stage.

The third-stage igniter was fired by a pressure switch, cocked at second-stage ignition, which closed as the second-stage motor chamber pressure decreased near burnout. After the third stage burned out, it coasted in free flight (with the instrument package) through apogee to impact.

RESULTS OF TWO FLIGHT TESTS

Trajectory

Figures 3 and 4 present values of altitude as a function of horizontal range as determined from Millstone Hill tracking radar for models 1 and 2, respectively. Launch angles used were 75° for model 1 and 80° for model 2.

Preflight estimates of altitude and range for a spherical, nonrotating earth are also shown in figures 3 and 4 for each model and tables 1 and 2 present estimates of the performance at ignition and burnout of each stage for both models. The calculated values were based on estimated weights and coast times supplied by the University of Michigan Research Institute and do not include wind effects. Considerable deviation from estimated to actual trajectory is shown for model 1. The deviation is smaller for model 2. Because of the possible combination of a number of parameters involved in establishing the actual model position at these altitudes, no attempt has been made herein to account for the deviations shown. A later section of the paper, however, does discuss the separate effects of payload, winds, coast time, and launch angle. It will also be shown that the deviations shown in figures 3 and 4 are not unreasonable when these effects are considered.

Figure 4 also shows altitude and range obtained from the NASA Wallops Station SCR 584 tracking radar set for the test of model 2. Due to the beacon malfunction in model 1 at take-off, radar tracking from NASA Wallops Station was questionable and is not shown for this test. Agreement between estimated and Wallops tracking trajectory data for model 2, however, was very good prior to second-stage ignition as can be seen by the comparative values of altitude, velocity, and Mach number shown in figure 5.

Drag

By using the values of velocity obtained from the Doppler velocimeter during the early portions of the tests, it was possible to determine total drag coefficients for models 1 and 2 during part of the coasting period following first-stage separation. This method consists essentially of differentiating velocity with respect to time (after applying corrections for flight-path angle and wind velocity) and computing drag with the accelerations thus obtained. These values of drag coefficient contain second-stage base drag and are based on the second-stage cross-sectional area of 1.48 square feet.

Values of drag coefficient for the coupled second and third stages during coast are plotted as a function of Mach number in figure 6 from the test of models 1 and 2. Agreement between the two sets of data is good between Mach numbers of 1.22 and 1.97. No values of drag coefficient could be obtained from model 1 at Mach numbers less than 1.22. Since the NASA Wallops Station trajectory data for model 1 were questionable (as mentioned previously), values of Mach number, dynamic pressure, and Reynolds number were calculated for that model with estimated values of altitude. Figure 7 shows the range of Reynolds numbers (based on a characteristic length of 1.0 foot) over which these drag data were obtained.

CALCULATED PERFORMANCE

This section of the paper presents the effects of some of the variables on the performance of the three-stage sounding rocket system discussed in the previous sections of this paper. The variable parameters considered are launch angle, coast time, and payload (where payload is defined as the weight of the package attached to the forward face of the third stage). The trajectory data assume a spherical, nonrotating earth with an inverse square gravitational field. A method of calculating this type trajectory is explained in chapter IX of reference 2. By making use of this calculated performance data at different values of these variables, it should be possible to evaluate, in general terms, the ability of this three-stage system to perform a desired test or experiment.

Table 3 shows the weight and thrust data for model 2 which were used in making all of the estimates discussed in this paper. The drag data used in making the trajectory calculations are shown in figures 8(a) and 8(b) $\left(\text{in terms of } \frac{\text{Drag}}{\text{Dynamic pressure}}\right)$ as a function of Mach number. In any adaptation of this system where the nose-cone shape, flare angle or fin size, or Reynolds number range differed from those considered in

this investigation, it would be necessary to reevaluate these drag values to apply to the particular vehicle and trajectory being considered. The same consideration is applicable to the weight data shown in table 3. The only weight variation considered in this section is that of payload; the effect on maximum altitude and range of varying component weights has not been evaluated. Values of thrust in table 3 are for the Honest John, Nike, and Recruit rocket motors at sea level and must be adjusted to account for the reduced static pressure at altitude. The estimates made in this paper have accounted for this effect by considering the change in the ratio of static pressure to chamber pressure at the altitudes involved. A discussion of the method used in estimating the thrust at altitude is given in Chapter 3 of reference 3.

Launch Angle

The calculated variation of maximum altitude and range with launch angle for a vehicle having an 81.5-pound payload and 25 seconds coast time is presented in figures 9(a) and 9(b), respectively. Maximum altitude increases as launch angle increases and it is evident that the maximum altitude would be obtained with a vertical launch. However, since the vehicle discussed does not contain guidance or destructor systems, launches in the vicinity of populated land areas should be limited to angles less than 90° (as in the case of models 1 and 2) as a safety precaution. Maximum range (fig. 9(b)) increases with launch angles to about 72° and decreases for greater launch angles. The effect of increasing launch angle between 72° and 90° is to increase maximum altitude and decrease maximum range.

Coast Time

Figures 10(a) and 10(b) show the effects of increasing coast time (time between first-stage burnout and second-stage ignition) for a vehicle with an 81.5-pound payload launched at angles of 80° and 85°. The effect of increased coast time is to increase the maximum altitude until some optimum coast time is reached (about 17 seconds for the 80° launch and 23 seconds for the 85° launch) and then decrease maximum altitude with further increase in coast time. Short coast periods have the effect of causing second-stage ignition to occur at lower altitudes and higher velocities than do the longer coast times, resulting in higher temperatures and loads. Therefore, before selecting the coast time to be used, temperatures and loads associated with the second- and third-stage components should be examined. Figure 10(b) shows that for both launch angles investigated, an increase in coast time causes an increase in maximum range.

Payload

The estimated variation of maximum altitude and range with payload weight is shown in figure 11 for a three-stage vehicle launched at 80° and 85° and having a 25-second coast time. Both maximum altitude and range are shown to decrease with increasing payload for both launch angles. Data for a five-stage vehicle of reference 1 at a launch angle of 80° are plotted for comparison in figure 11(a).

Estimates of velocity at third-stage burnout are plotted as a function of payload in figure 12. This maximum velocity was found to be almost unaffected by changes in launch angle or coast time, and depends almost entirely upon the payload carried by the third stage. Payload weight, however, was found to have an insignificant effect upon velocity at first- and second-stage burnout.

L
6
1
0

Effects of Wind

Figure 13 shows the effect of one wind profile on the trajectory of a model launched at 80° with a 25-second delay between first-stage burnout and second-stage ignition (coast time) and an 81.5-pound payload. The wind data tabulated on this figure are the same as those discussed in reference 1 and are a series of straight-line approximations to a profile that could be encountered in the eastern United States. For any operational launching, of course, the wind profile applicable to the particular day and site location should be used rather than the tabulated wind velocities of figure 13.

Large deviations in trajectory are shown at the higher altitudes, although most of the angular variation was found to occur during first-stage thrusting. These wind effects in terms of maximum altitude and range are shown in figure 14, where a headwind is seen to decrease maximum altitude and increase maximum range and a tailwind increases maximum altitude and decreases range.

Very large differences in predicted altitude and range are seen to result from small changes in flight-path angle at third-stage burnout due to the horizontal headwind or tailwind profile used. The values shown in figure 14 indicate that the deviation in figures 3 and 4 between "no wind" estimates and actual model trajectory is not unreasonable since radiosonde data, taken at the time of launching, indicate that both test vehicles during the early portions of the tests experienced a tailwind component. For operational launchings where altitude and range are critical, account must be taken of the winds to be encountered.

Static Stability

Estimates of center-of-pressure and center-of-gravity location, from launch to third-stage burnout, were made for this sounding rocket system boosting an 81.5-pound payload. These estimates are presented as a function of Mach number in figure 15. It can be seen from figure 15 that, although the vehicle was stable at all Mach numbers, the static margin of the third stage was less than for the first and second stages. Lighter payloads would further decrease the static stability of the third stage. Consequently, third-stage stability must be considered when adapting this sounding rocket system to a specific test with a payload less than 81.5 pounds. No artificial stabilization for the third stage was employed on the vehicles tested and it is possible that tumbling or spinning occurred at the higher altitudes. Tumbling at low density altitudes should have no appreciable effect on the trajectory of the burned-out third stage, but it could be undesirable for certain types of tests in which case spin stabilization of this stage might be necessary.

Booster Trajectories

Estimates were made to determine the trajectories followed by the expended first- and second-stage boosters after separation. The conditions chosen as starting points for these estimates were those associated with a vehicle launched at 80°, with a coast time of 25 seconds. The calculated drag data used in making these estimates are shown in figure 8(b). Wind effects were not considered. The following table presents the maximum altitude and impact range of the stages:

	Maximum altitude (nautical miles)	Impact range (nautical miles)
Burned-out first stage	5.8	3.3
Burned-out second stage	18.3	17.5

CONCLUDING REMARKS

Two successful operational launchings of a three-stage solid-fuel sounding rocket system have been made. This system has demonstrated the capability of carrying an 81.5-pound payload to an altitude of 253 nautical miles. Estimates have been made which show that the maximum altitude and range of such a system will be dependent on the payload weight, launch

angle, and delay time between first-stage burnout and second-stage ignition used in a particular test. Wind-velocity profile at the launching site was also shown to have an effect on the maximum altitude and range.

Langley Research Center,
National Aeronautics and Space Administration,
Langley Field, Va., August 4, 1959.

REFERENCES

1. Swanson, Andrew G.: A Five-Stage Solid-Fuel Sounding-Rocket System. NASA MEMO 3-6-59L, 1959.

2. Kooy, J. M. J., and Uytenbogaart, J. W. H.: Ballistics of the Future. McGraw-Hill Book Co., Inc., 1946.

3. Sutton, George P.: Rocket Propulsion Elements. Second ed., John Wiley & Sons, Inc., 1957.

TABLE 1.- ESTIMATED PERFORMANCE OF MODEL 1 AT IGNITION AND BURNOUT OF EACH STAGE

[Calculated maximum altitude, 189 nautical miles]

	First stage		Second stage		Third stage	
	Ignition	Burnout	Ignition	Burnout	Ignition	Burnout
Altitude, ft	0	6,255	39,271	46,119	46,119	57,139
Horizontal range, ft	0	1,959	15,484	19,985	19,985	27,378
Velocity, ft/sec	0	2,306	865	4,339	4,339	10,495
Flight-path angle, deg	75.00	72.05	57.78	56.24	56.24	55.99
Time, sec	0	5.20	30.20	33.40	33.40	35.20

TABLE 2.- ESTIMATED PERFORMANCE OF MODEL 2 AT IGNITION AND BURNOUT OF EACH STAGE

[Calculated maximum altitude, 239 nautical miles]

	First stage		Second stage		Third stage	
	Ignition	Burnout	Ignition	Burnout	Ignition	Burnout
Altitude, ft	0	6,413	40,741	48,246	48,246	60,461
Horizontal range, ft	0	1,318	10,466	13,593	13,593	18,777
Velocity, ft/sec	0	2,303	845	4,322	4,322	10,523
Flight-path angle, deg	80.00	78.01	68.16	67.06	67.06	66.89
Time, sec	0	5.20	30.20	33.40	33.40	35.20

TABLE 3.- ESTIMATED WEIGHT AND THRUST VALUES FOR MODEL 2 USED IN CALCULATING PERFORMANCE PARAMETERS

[Linear variations were used between points tabulated]

Flight phase	Time from launch, sec	Weight, lb	Thrust at sea level, lb
First-stage thrusting	0 4.20 5.20	5,778 3,978 3,728	84,000 84,000 0
Stages 2 and 3 coasting	5.20 30.20	1,696 1,696	0 0
Second-stage thrusting	30.20 33.00 33.40	1,696 1,009 956	42,500 50,000 0
Third-stage thrusting	33.40 34.95 35.20	435 194 179	37,000 30,000 0
Third-stage coasting	35.20 800.00	179 179	0 0

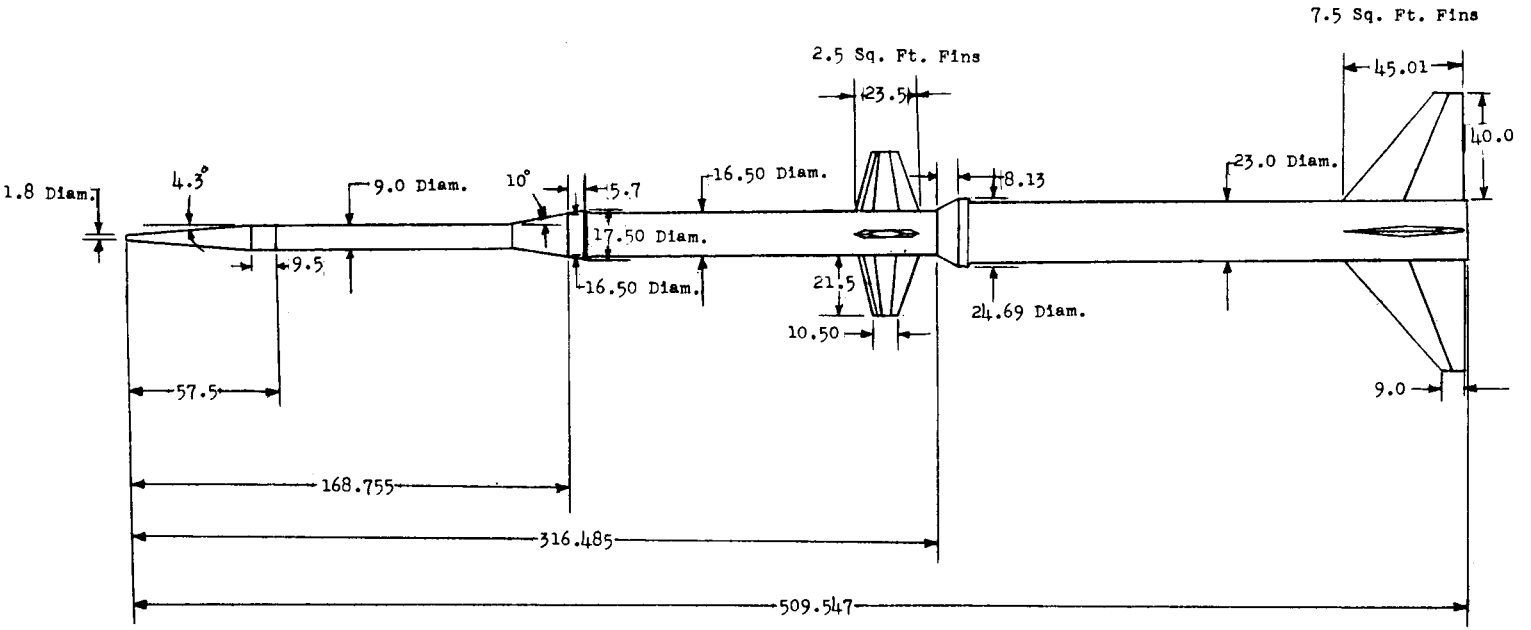

Figure 1.- The second three-stage vehicle tested. All dimensions are in inches.

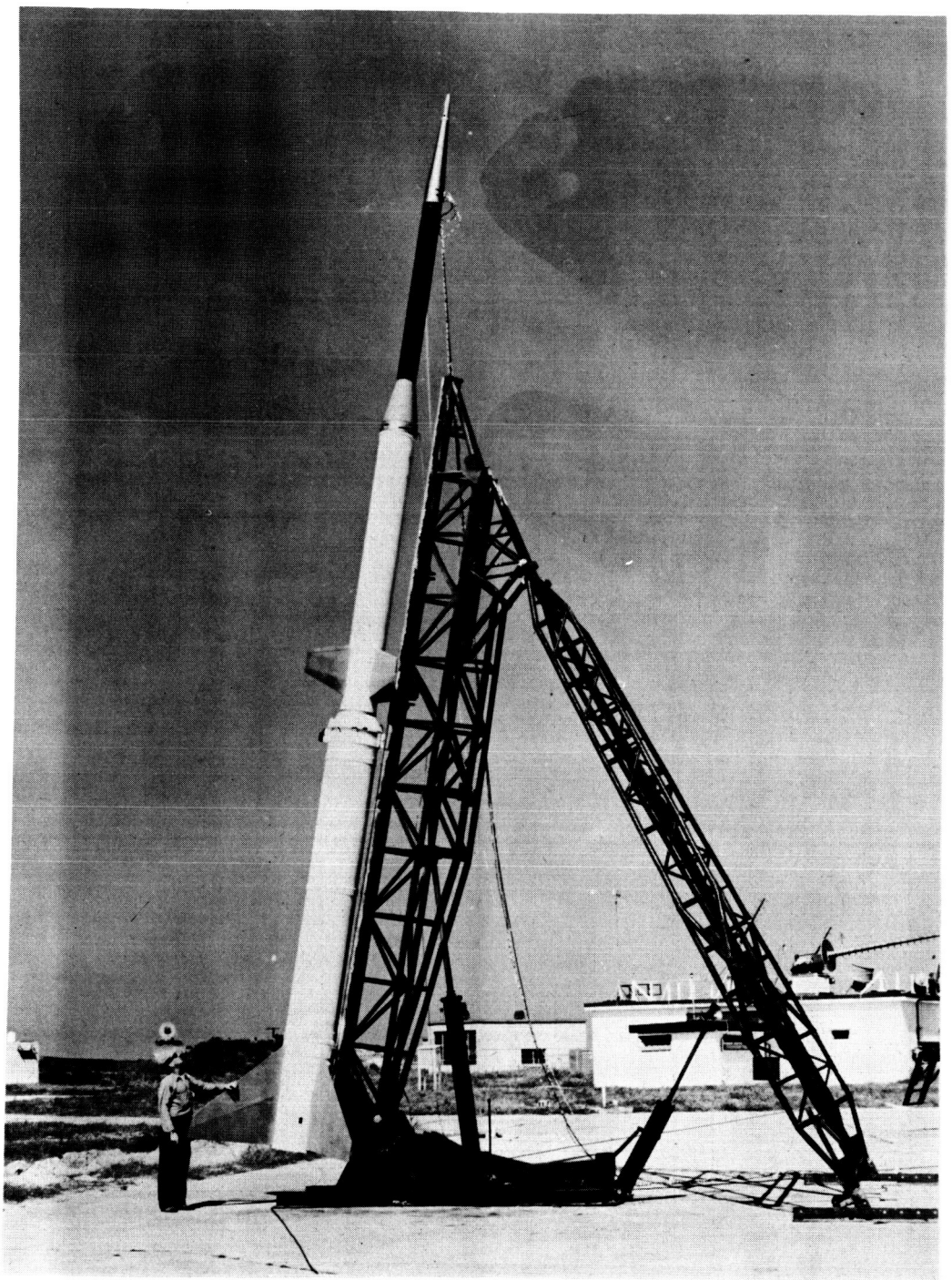

L 58-4474

Figure 2.- The second three-stage vehicle on the launcher.

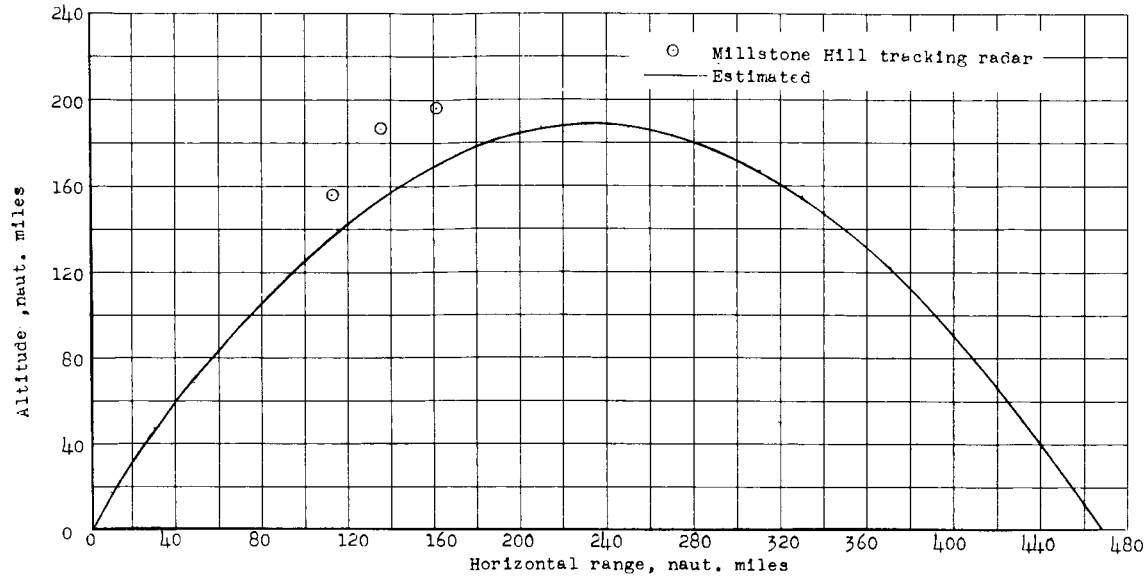

Figure 3.- Flight test data and estimated trajectory for model 1. Launch angle = 75°.

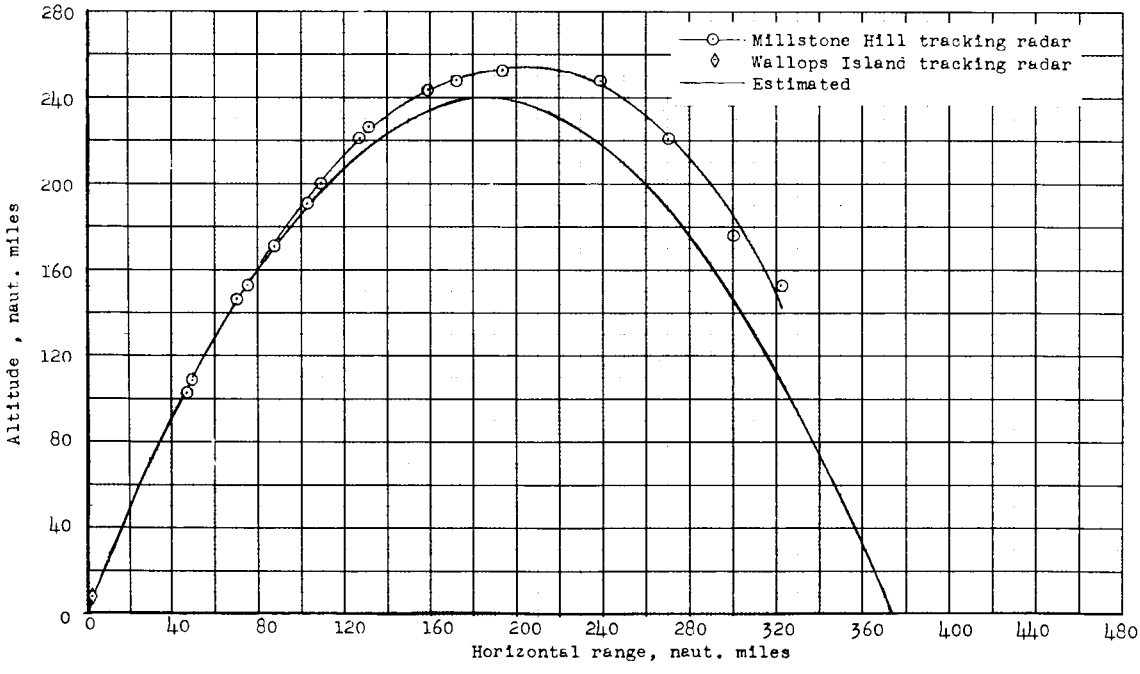

Figure 4.- Flight test data and estimated trajectory for model 2. Launch angle = 80°.

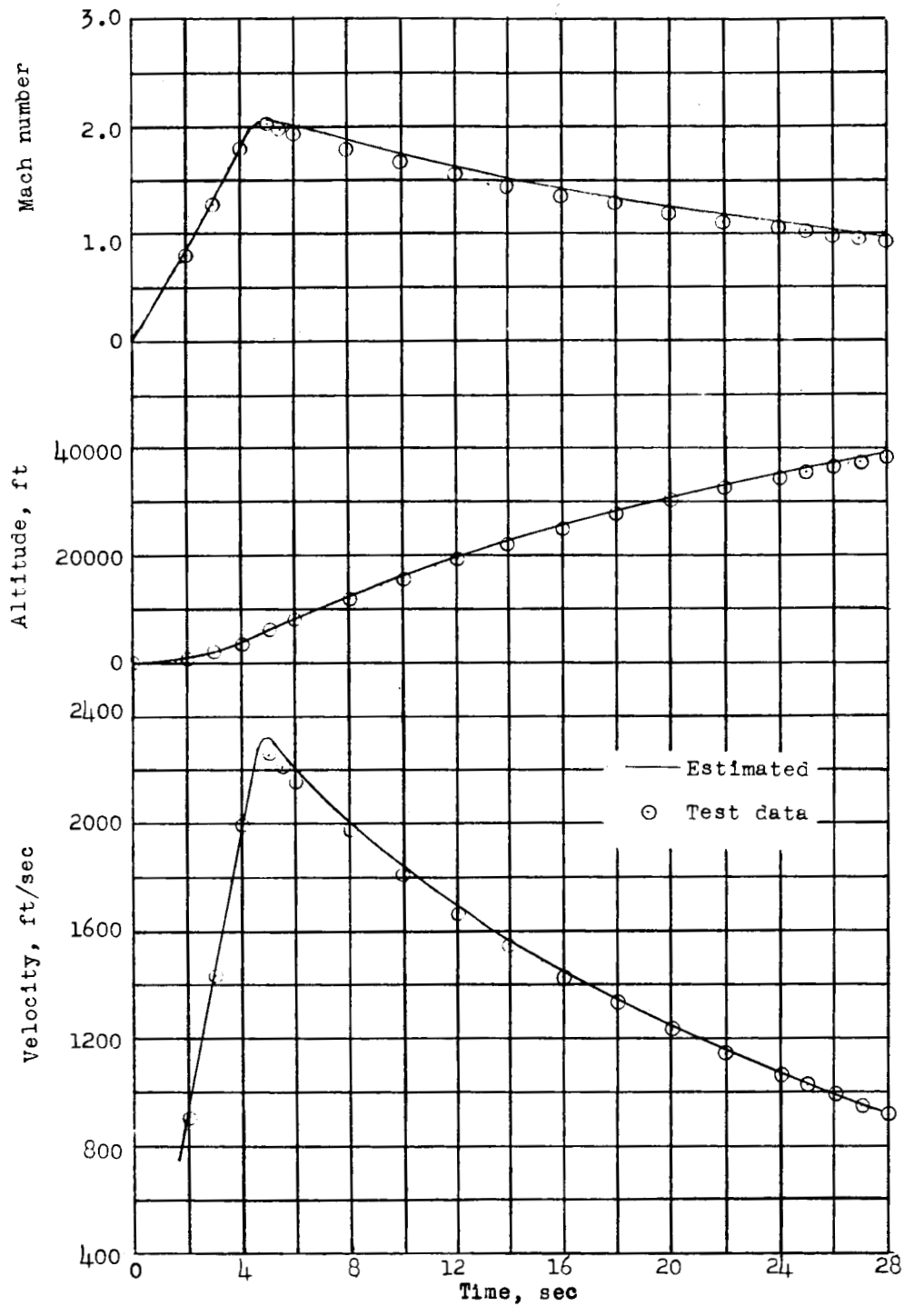

Figure 5.- Comparison of estimated and measured Mach number, altitude, and velocity for model 2. Launch angle = 80°; coast time = 25 sec.

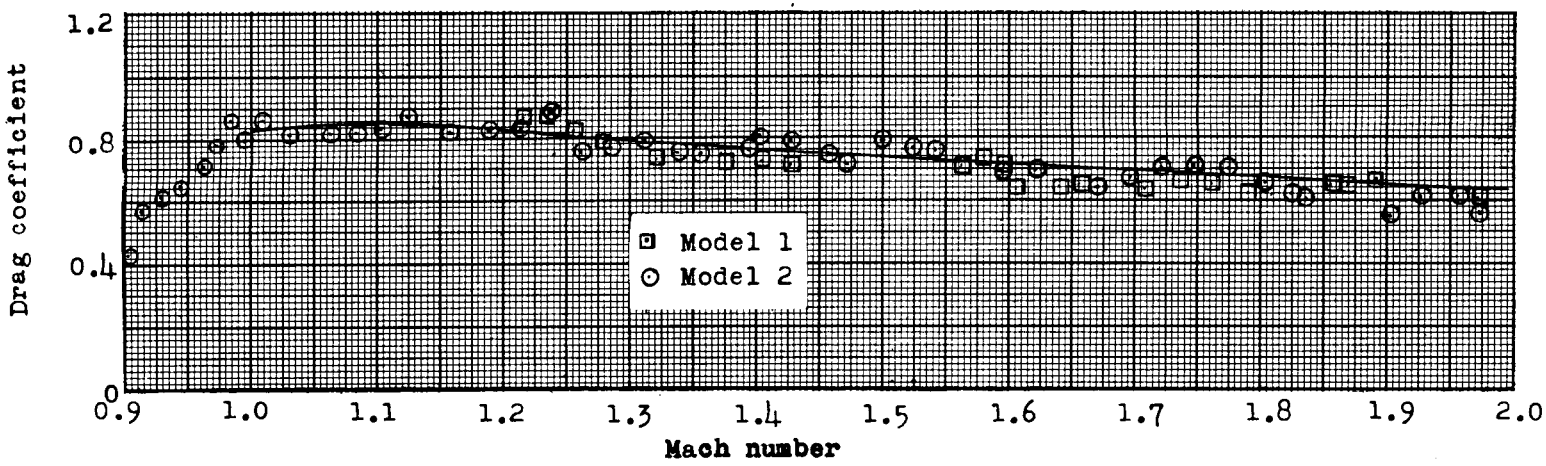

Figure 6.- Variation of drag coefficient with Mach number for models 1 and 2 during coasting period of stages 2 and 3 based on second-stage cross-sectional area of 1.48 square feet.

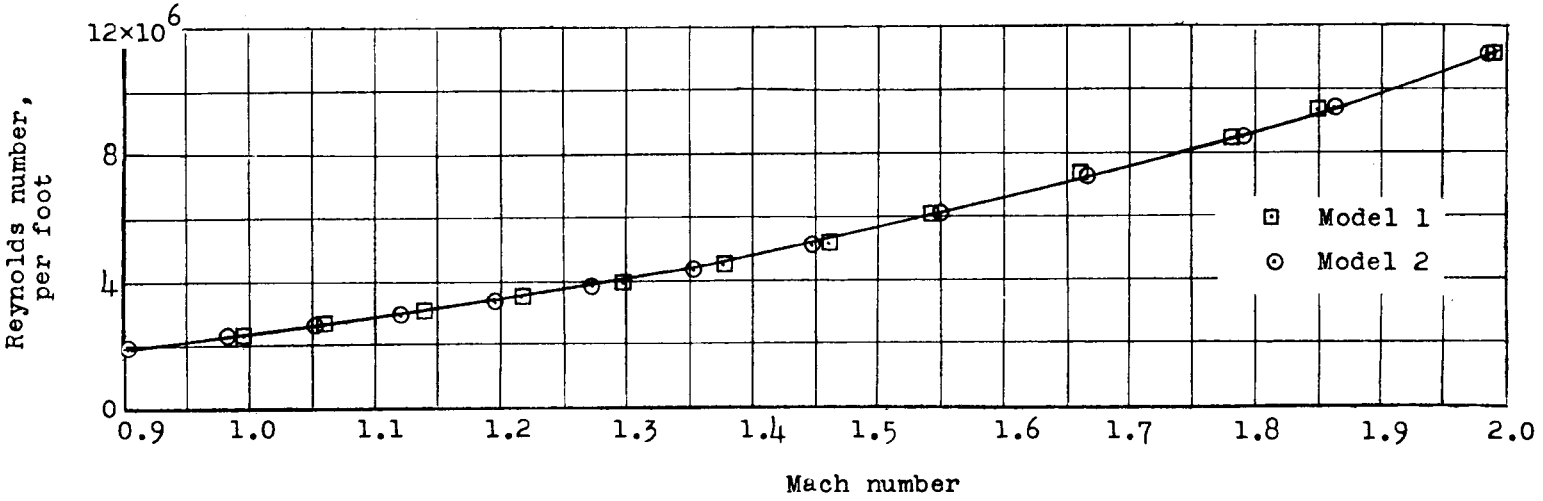

Figure 7.- Variation of Reynolds number with Mach number for models 1 and 2 during coasting period of stages 2 and 3.

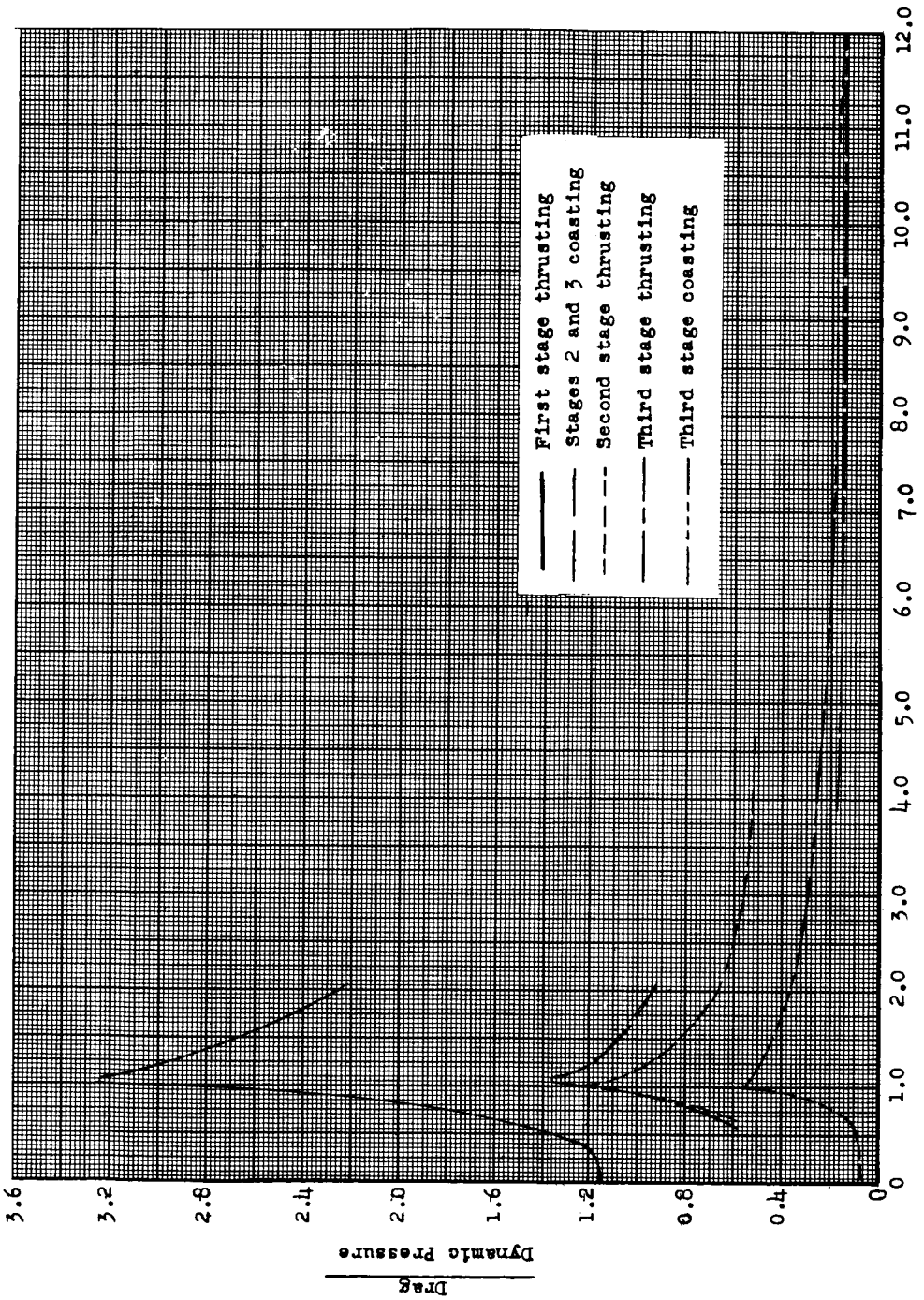

(a) Values for model 2 used in making performance estimates.

Figure 8.- Estimated drag values.

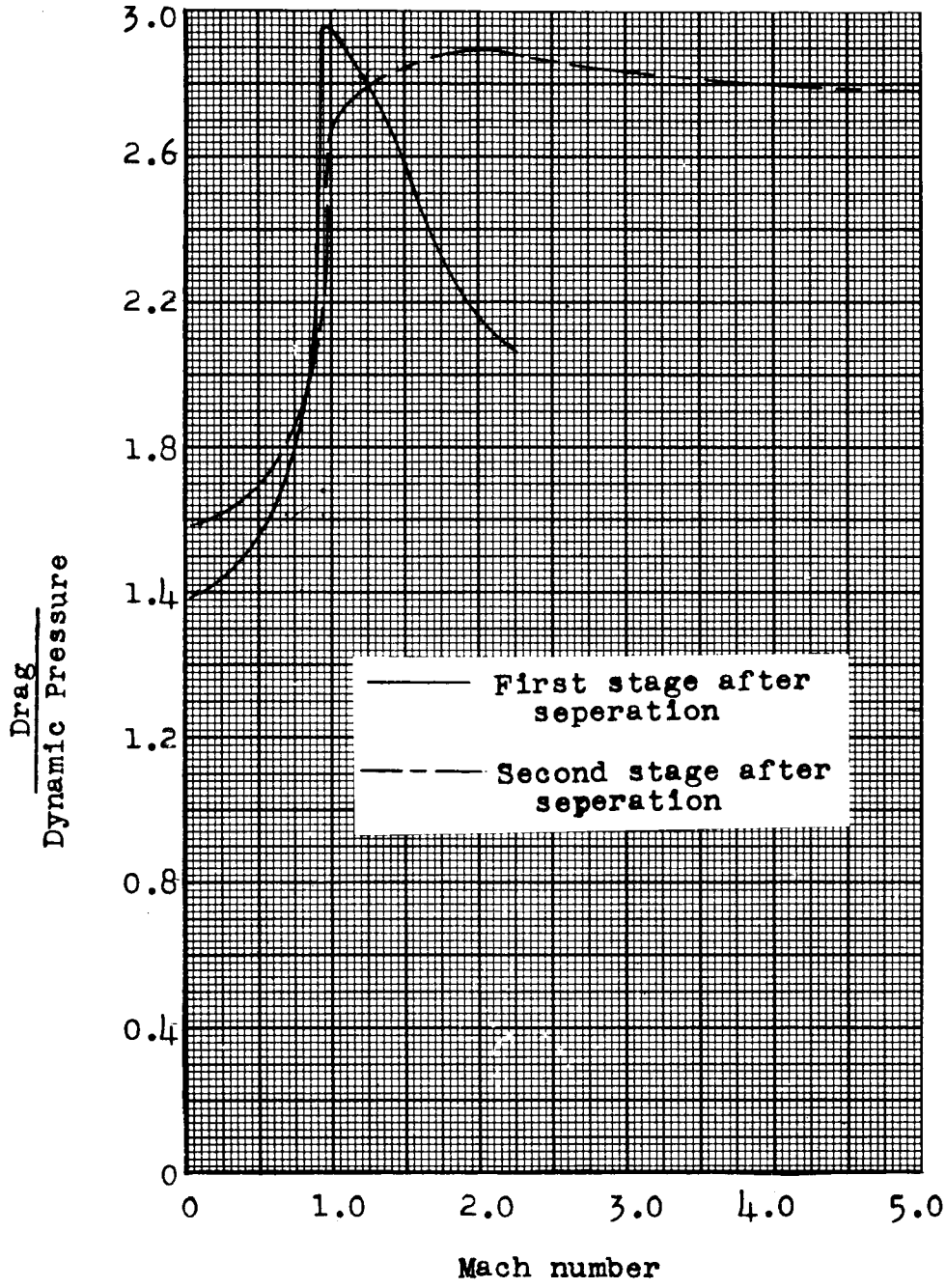

(b) Values used to calculate expended first- and second-stage booster trajectories.

Figure 8.- Concluded.

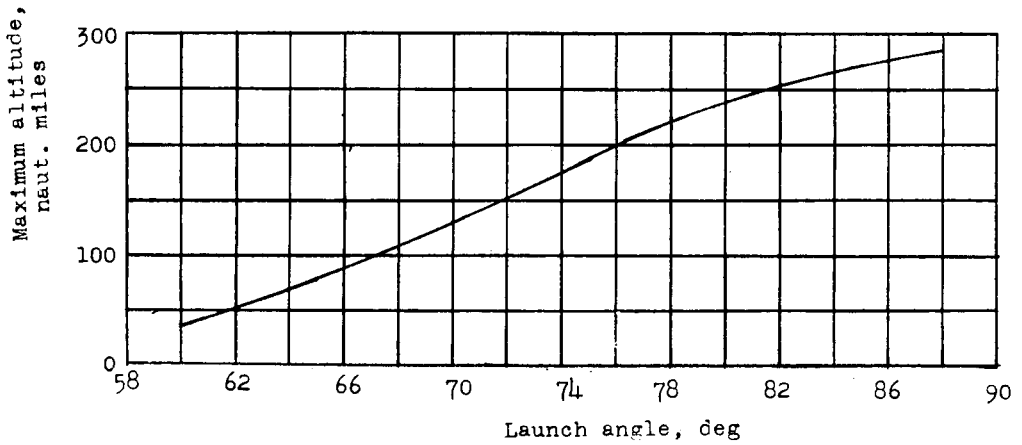

(a) Maximum altitude.

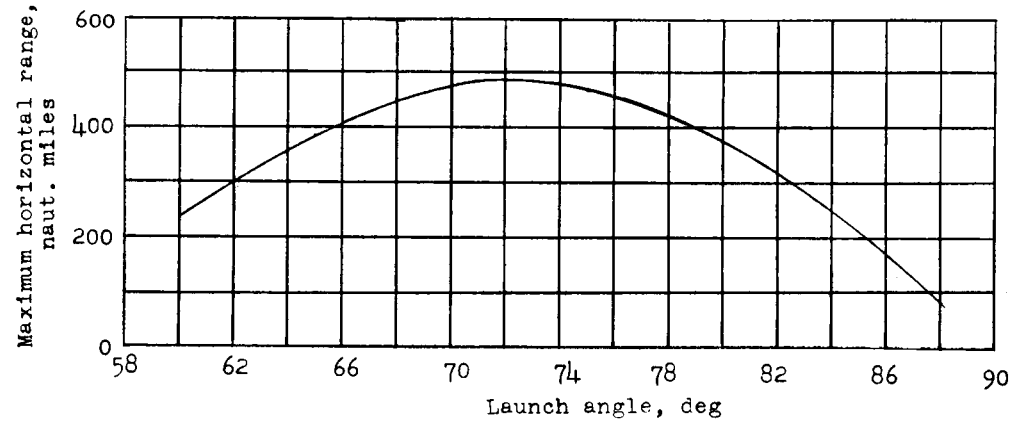

(b) Maximum horizontal range.

Figure 9.- Variation of maximum altitude and range with launch angle. (81.5-pound payload and 25-second coast period)

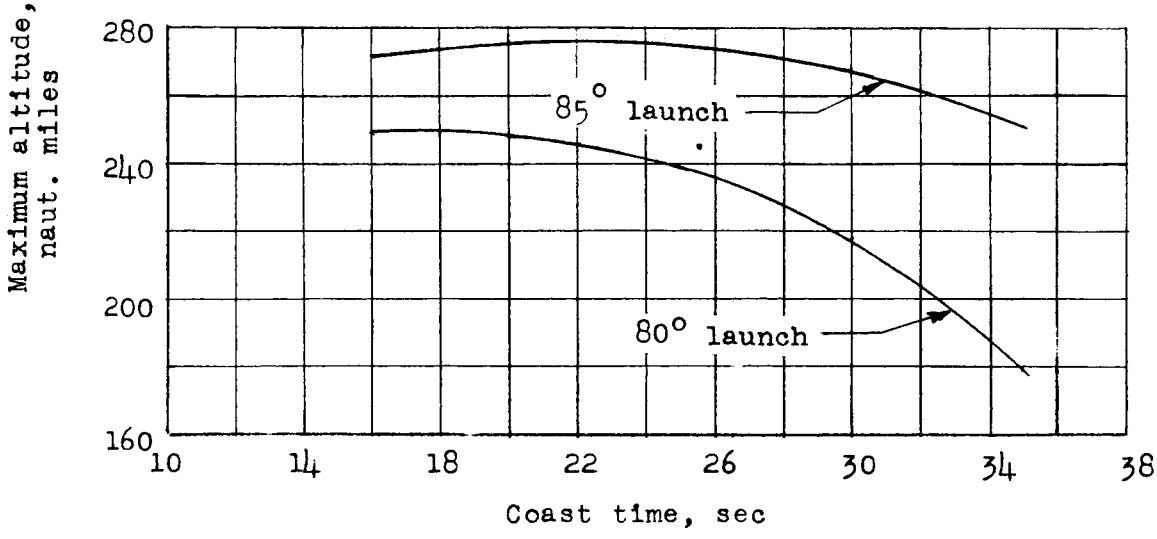

(a) Maximum altitude.

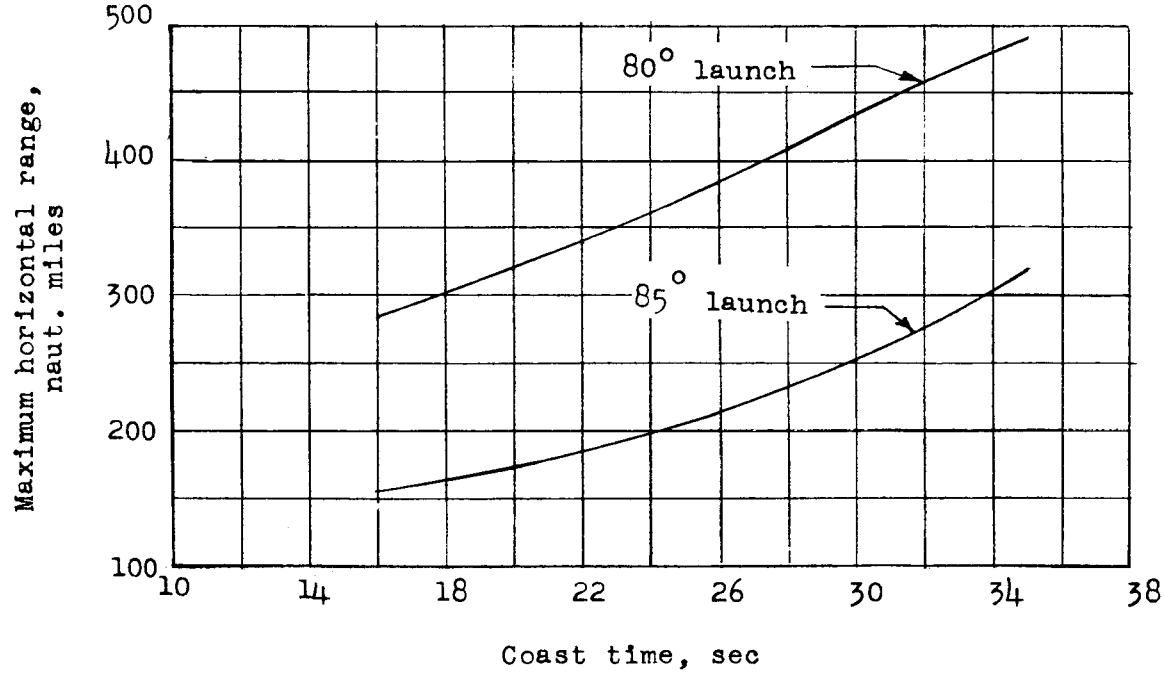

(b) Maximum horizontal range.

Figure 10.- Variation of maximum altitude and range with coast period. (81.5-pound payload)

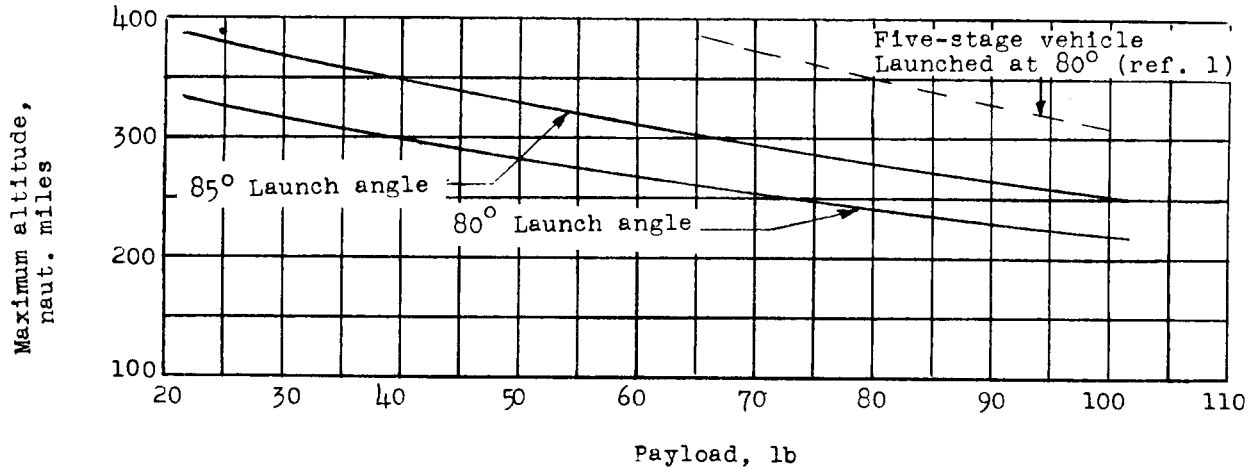

(a) Maximum altitude.

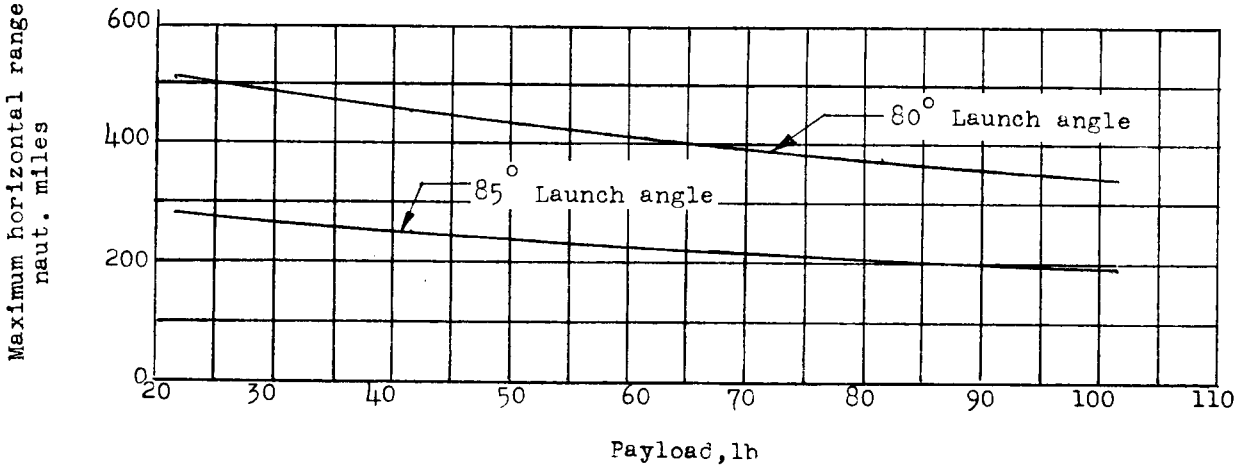

(b) Maximum horizontal range.

Figure 11.- Variation of maximum altitude and range with payload. (25-second coast period)

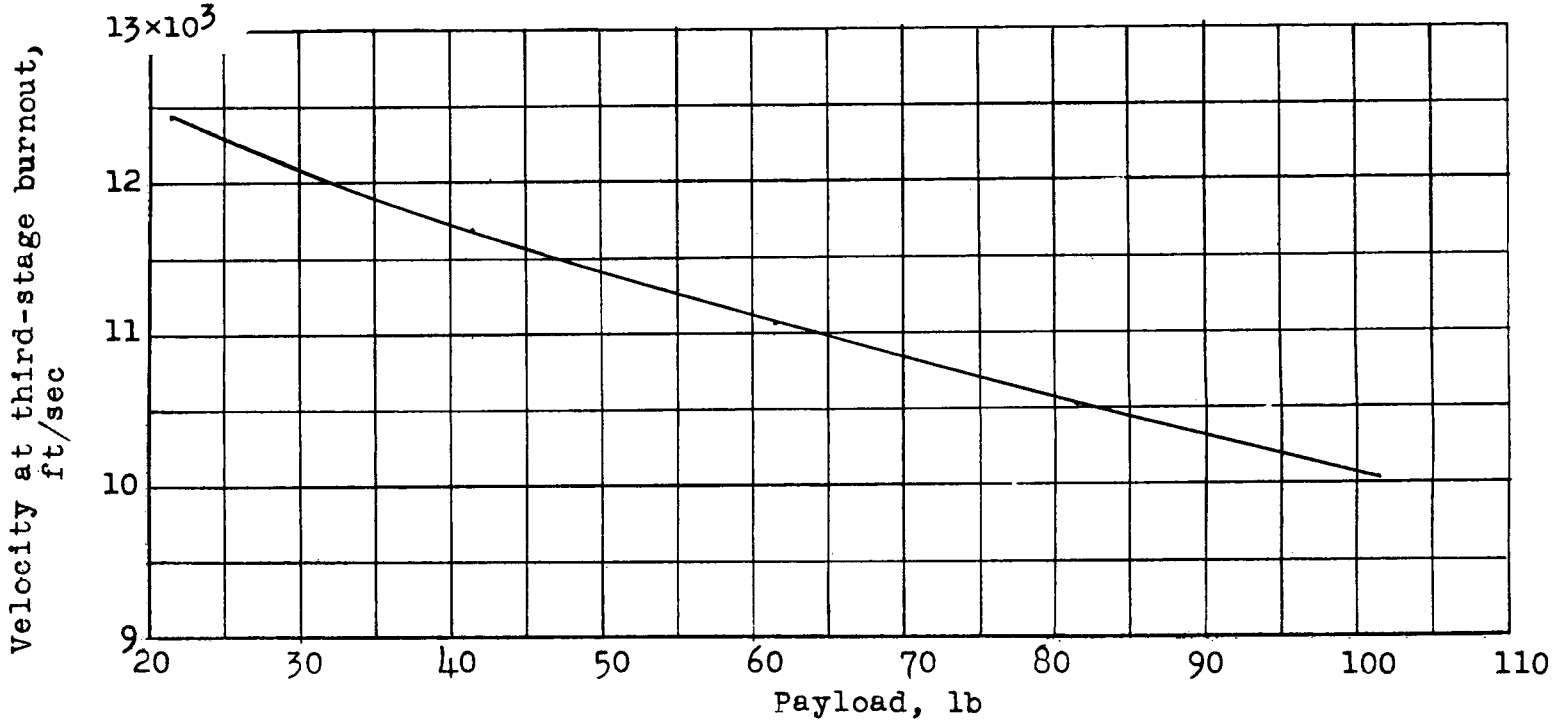

Figure 12.- Variation of velocity at third-stage burnout with payload. (Launch angle = 80° and coast time = 25 sec.)

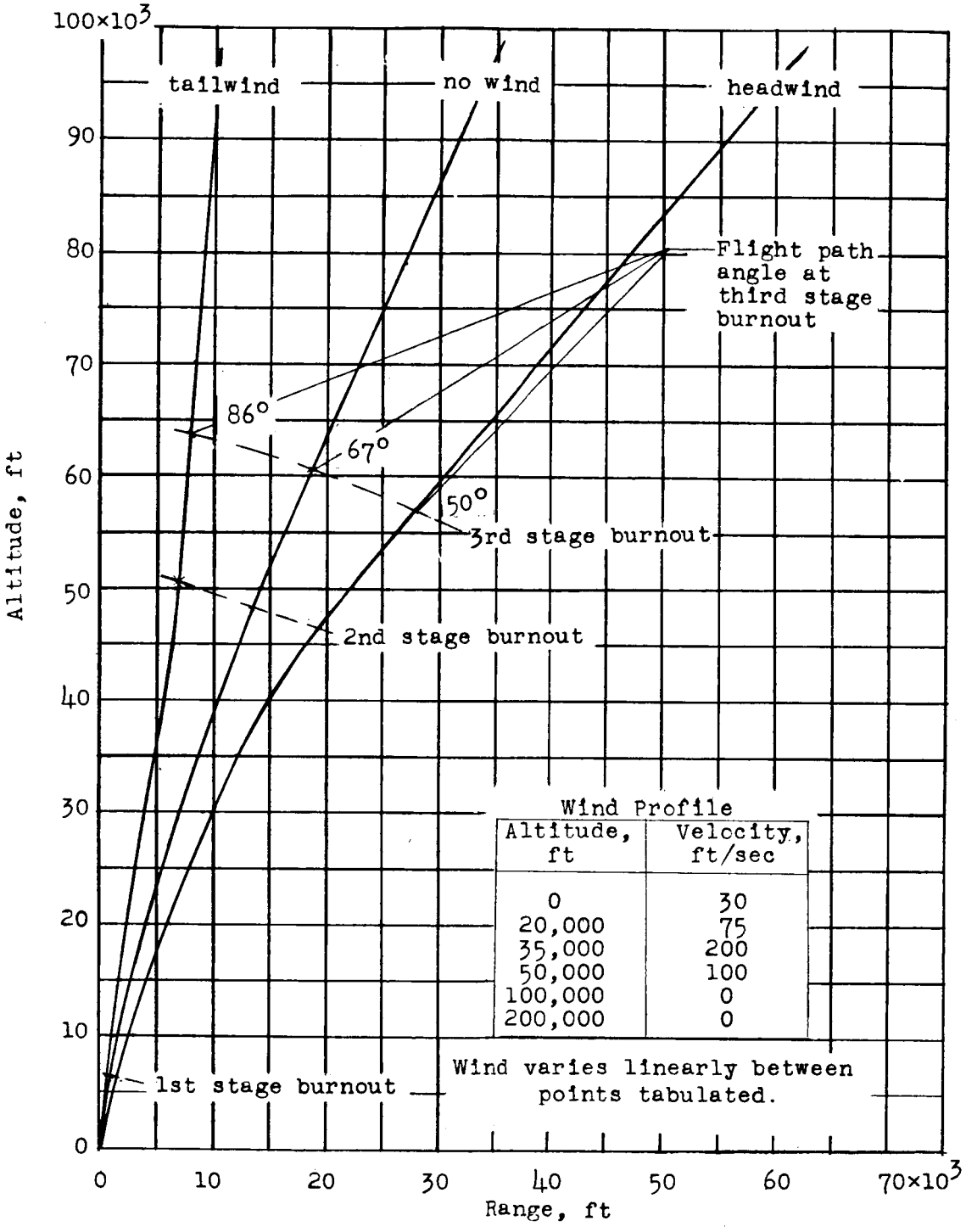

Figure 13.- Effects of constant direction horizontal winds on flight-path angle. Launch angle = 80°; coast time = 25 sec; payload = 81.5 lb.

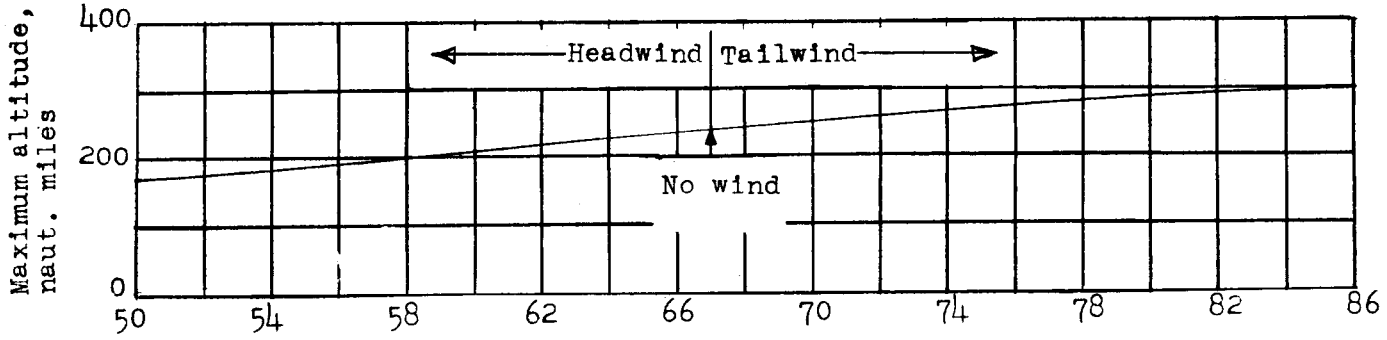

(a) Maximum altitude.

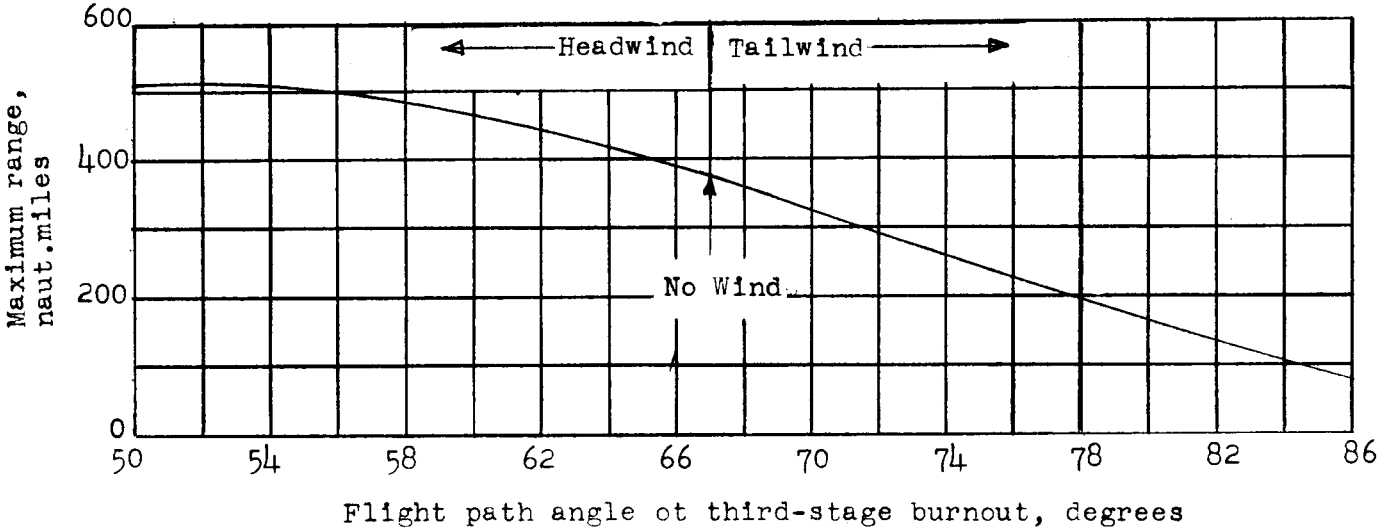

(b) Maximum range.

Figure 14.- Variation of maximum altitude and range with flight-path angle at third-stage burnout.

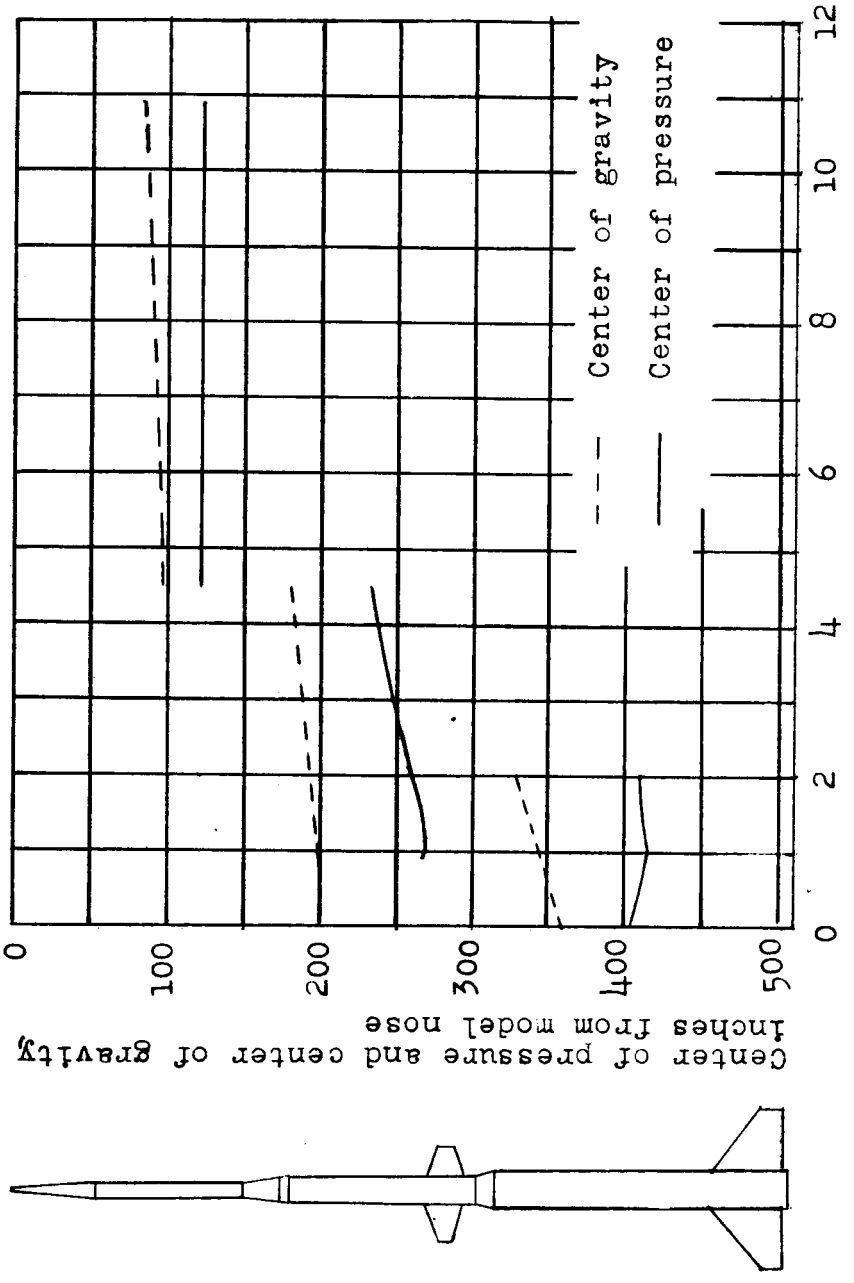

Figure 15.- Estimated static margin from launch to third-stage burnout.